Liquid Crystals
Publication details, including instructions for authors and subscription information:
http://www.informaworld.com/smpp/title~content=t713926090

Polar nematic *trans*-4-substituted-cyclohexyl (*E*)-alk-2-enoates The influence of dipoles and double bonds on the transition temperatures and other physical properties

S. M. Kelly[a]; M. Schadt[a]; H. Seiberle[a]
[a] F. Hoffmann-La Roche Ltd., Dept. RLCR, Basle, Switzerland

To cite this Article Kelly, S. M. , Schadt, M. and Seiberle, H.(1995) 'Polar nematic *trans*-4-substituted-cyclohexyl (*E*)-alk-2-enoates The influence of dipoles and double bonds on the transition temperatures and other physical properties', Liquid Crystals, 18: 4, 581 — 594

To link to this Article: DOI: 10.1080/02678299508036661

URL: http://dx.doi.org/10.1080/02678299508036661

LIQUID CRYSTALS, 1995, VOL. 18, NO. 4, 581–594

Polar nematic *trans*-4-substituted-cyclohexyl (*E*)-alk-2-enoates

The influence of dipoles and double bonds on the transition temperatures and other physical properties

by S. M. KELLY*, M. SCHADT and H. SEIBERLE
F. Hoffmann-La Roche Ltd., Dept. RLCR, CH-4002 Basle, Switzerland

(*Received 26 June 1994; accepted 8 August 1994*)

As part of a systematic study of the factors affecting nematic phase formation, the influence of introducing dipoles (in the form of oxygen, carbonyl and carboxy groups) and steric restrictions (in the form of carbon–carbon double bonds) in various positions, configurations and combinations in a model system (4-[*trans*-4-pentylcyclohexyl]benzonitrile) has been investigated. On the basis of these results, we have introduced an ester group *and* a carbon–carbon double bond with a *trans*-configuration (*E*) into the terminal alkyl chain attached to the cyclohexyl ring of a variety of two- and three-ring nematic mesogens of positive dielectric anisotropy. This is a new combination of a polar ester group (dipole effect) and the added rigidity imposed by the double bond (steric effect). Most of the new (*E*)-alk-2-enoates containing two rings in the molecular core possess high melting points. Only a few two-ring esters exhibit a nematic phase, although the clearing point of those esters exhibiting mesomorphic behaviour was high. The corresponding three-ring (*E*)-alk-2-enoates incorporating an additional phenyl or cyclohexane ring also possess high melting and clearing points, as well as wide nematic ranges. No smectic mesophases could be observed for any of the (*E*)-alk-2-enoates synthesized. Comparisons with the corresponnding derivatives incorporating either just an ester group, or just a carbon–carbon double bond in the same position indicate that synergetic effects lead to higher clearing points than would otherwise have been expected. The new (*E*)-alk-2-enoates possess a surprisingly moderate viscosity for esters. The high value of the elastic constant ratio k_{33}/k_{11} is of advantage for mixtures designed for supertwisted nematic LCDs.

1. Introduction

During the past 20 years, attempts to optimize the physical properties of polar nematogens for field-effect liquid crystal displays (LCDs) [1–11] have concerned themselves with varying the rings in the core [12–20], the terminal substituents [17–24] and the central linkages [23–28]. The terminal aliphatic chains have been modified by the introduction of hetero-atoms (for example, S, N, Si, O, [29–32]) and carbon–carbon double bonds (for example, [33–41]). This is exemplified by the data collated in table 1, where a series of *trans*-4-substituted-cyclohexylbenzonitriles bearing a chain of fixed length (five units) incorporating either an oxygen atom and/or a carbon–carbon double bond of defined configuration in differing positions, as well as the reference compound (**1**) [19], is shown. The position of a hetero-atom or a carbon–carbon double bond is of critical importance [29–41]. This is clearly shown by considering the series of ethers (**2–5**) which differ only in the position of the oxygen atom [39]. Only the methoxypropyl-substituted-benzonitrile (**5**), with an oxygen atom at some distance from the core, exhibits a nematic phase [39]. However, as the melting point is higher (+ 22°C) than that of the unsubstituted benzonitrile (**1**), the nematic range is narrower. The other ethers (**2–4**) do not exhibit an observable nematic phase [39]. As the angle made by the carbon–oxygen–carbon bond (CH_2OCH_2) is very similar to that with a methylene unit instead of the oxygen atom ($CH_2CH_2CH_2$), it must be assumed that the effects of the oxygen atom on the clearing point is primarily of a polar and not a steric nature (i.e. the chain conformation distribution in each case should be essentially similar). Dramatic differences in the liquid crystal transition temperatures of the benzonitriles (**6–12**) with a carbon–carbon double bond (C=C) in the terminal chain are also observed [36]. The elastic and dielectric constants also differ greatly, which is of direct commercial and technological relevance for LCDs [35, 36]. These results were shown to agree qualitatively with the results obtained from molecular modelling, not of single compounds, but of ensembles of molecules [40]. Steric effects due to different configurations of the terminal chain were

---

* Author for correspondence.

0267-8292/95 $10·00 © 1995 Taylor & Francis Ltd.

Table 1. Transition temperatures for the 4-(*trans*-4-substituted cyclohexyl)benzonitriles below.

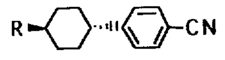

Compound	*R*	C–N/I/°C	N–I/°C	ΔT_{N-I}/°C	Reference
1		30	55	25	[19]
2		60	—	—	[39]
3	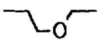	23	—	—	[39]
4	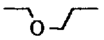	42	—	—	[39]
5		52	55	3	[39]
6	(E) 	16	59	43	[36]
7	(Z) 	—	[− 144]	—	[36]
8	(E) 	16	[− 67]	—	[36]
9	(Z) 	− 8	[− 54]	—	[36]
10	(E) 	60	74	14	[36]
11	(Z) 	33	(− 14)	—	[36]
12		30	(10)	—	[36]
13	(E) 	84	—	—	[39]
14	(E) 	66	(59)	—	[43]
15	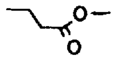	56	—	—	
16	(E) 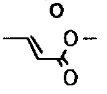	128	(119)	—	

( ) Represents a monotropic transition temperature.
[ ] Represents a virtual (extrapolated) transition temperature.

cited as the prime reason for the very large differences in the observed transition temperatures [35, 36]. The effect of combining these two functional groups (one exerting polar, the other steric effects) on the mesogenic tendencies of compounds is shown by reference to the ethers (**13** and **14**). For one ether (**13**) [39], no liquid crystal behaviour could be determined, while for the second ether (**14**) [42] a monotropic nematic phase could be detected at a temperature higher than that of the reference substance (**1**). It is clear that the interaction between steric and attractive forces is complicated.

Systematic studies of the effect of introducing these two groups (i.e., an oxygen atom and a double bond) into the side chain of a wide variety of polar (for example, **14**, see table 1) and weakly polar nematogens have shown [42–44] that incorporating certain configurations of these groups (for example, (*E*)-methoxypropenyl-substituted ($CH_3OCH_2CH{=}CH$) compounds) can lead to high nematic isotropic transition temperatures (T_{NI}) and wide-range nematic phases. Comparisons with the corresponding derivatives incorporating either just an oxygen atom, or just a carbon–carbon double bond in the same position showed that these effects were not purely additive. This was partially due to the low smectic transition temperatures observed. Such (*E*)-methoxypropenyl-substituted compounds were often found to be useful components for nematic mixtures, especially where a wide temperature range is required [42–44].

These studies have now been extended to terminal chains containing an *ester* group (COO) and a carbon–carbon double bond, i.e., the (*E*)-alk-2-enoyloxy group ($C_nH_{2n+1}CH{=}CHCOO$) and especially the (*E*)-2-butenoyloxy moiety ($CH_3CH{=}CHCOO$). It has recently been shown that (aromatic) pyrimidinyl- and pyridinyl-phenyl esters of (*E*)-alk-2-enoic acids exhibit high

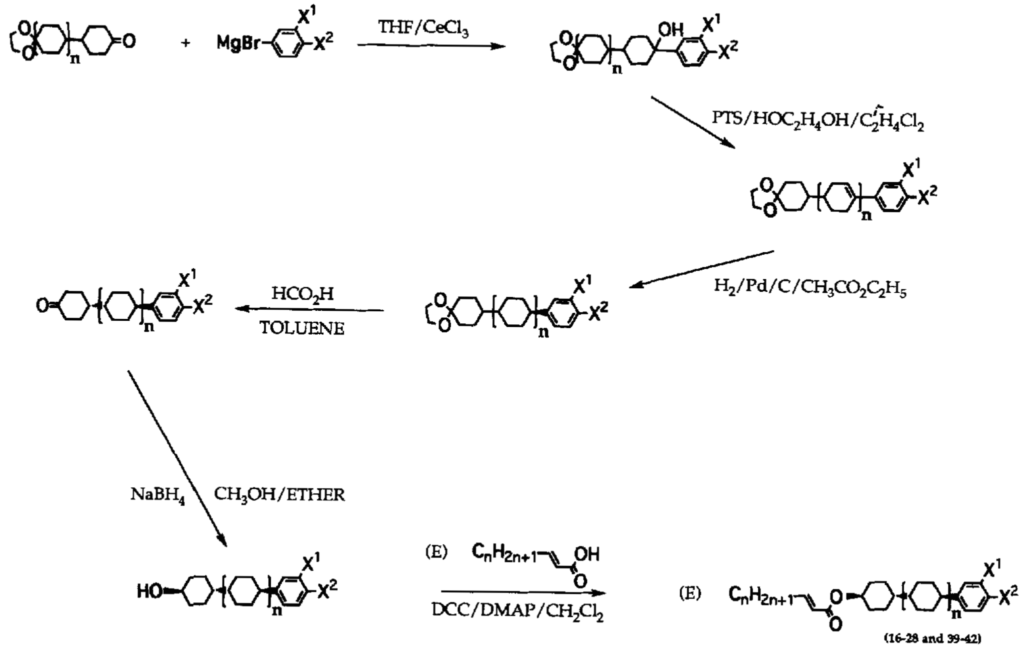

Scheme 1.

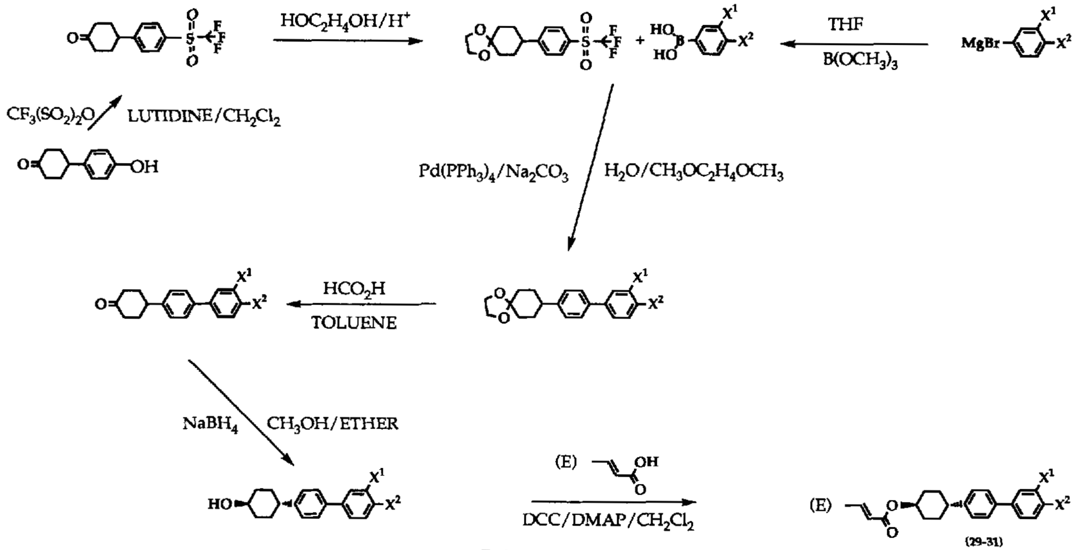

Scheme 2.

nematic transition temperatures [45] for two-ring systems. This effect has already been observed for a limited number of other aromatic esters [46, 47] and has been explained in terms of a high degree of polarizability due to conjugation between the carboxy (ester) group, the carbon–carbon double bond and the benzene ring [46]. Similar effects have recently been observed for a range of related aromatic phenylpyrimidine and phenylpyridine ethers [48–51], although primarily steric effects were invoked to explain the effects on the smectic transition temperatures. Initial results with (*E*)-but-2-enoic (crotonic) acid were very promising (for example, **16**, see table 1), especially when compared to the corresponding aliphatic esters without an additional carbon–carbon double bond (for example, **15**, see table 1). The fact that the butanoate (**15**) without a carbon–carbon double bond is not mesomorphic, while the corresponding (*E*)-but-enoate (**16**) with a *trans*-carbon–carbon double bond exhibits a clearing point (N–I) at a much higher temperature than that of the reference benzonitrile (**1**) shows how complex the relationship

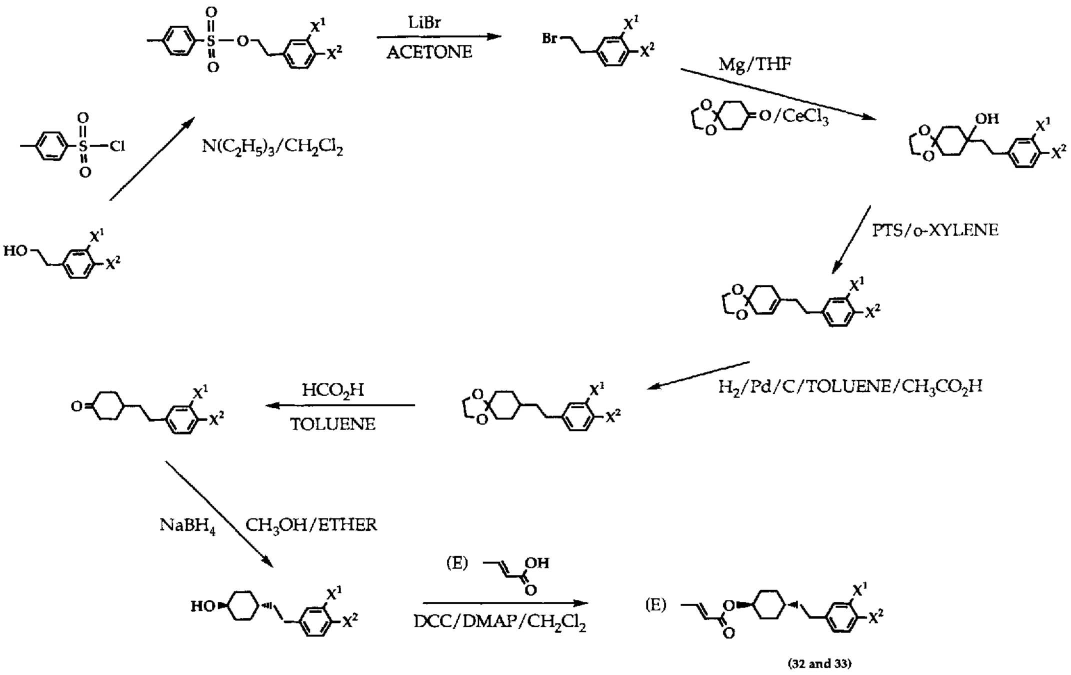

Scheme 3.

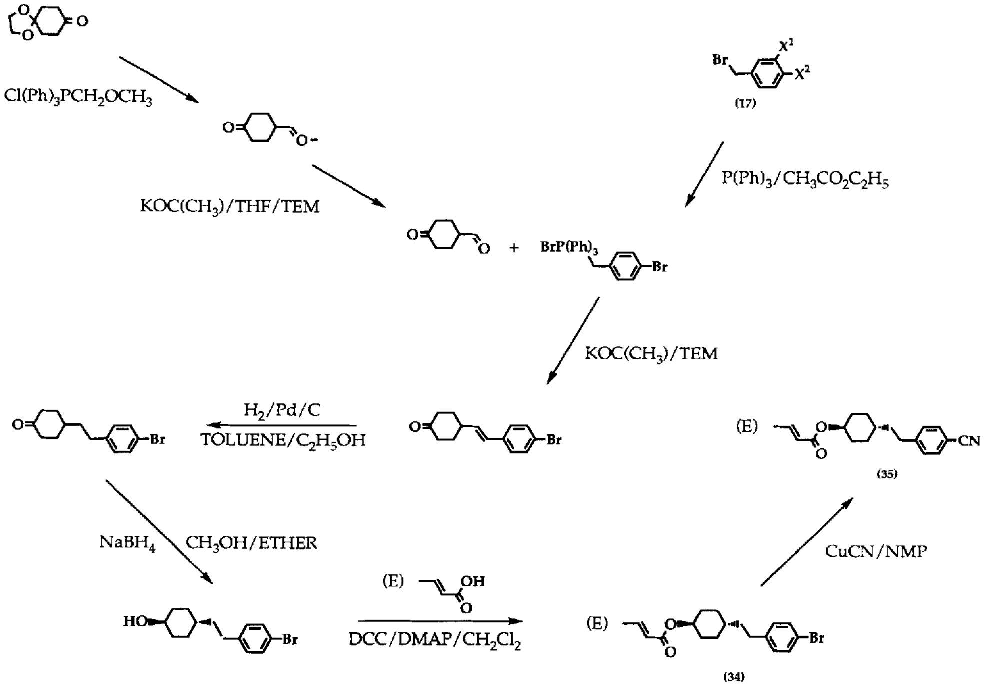

Scheme 4.

between structure and transition temperatures can be. Systematic studies such as these investigating the influence of polar and steric effects on the liquid crystal transition temperatures of model systems may help to elucidate the relative merits of the Maier–Saupe theory [52], the various Hard Rod theories [53] and Combined theories [54–57] for the nematic mesophase. Similar results to those reported here for polar mesogens have also been found for weakly polar mesogens of related structure [58, 59].

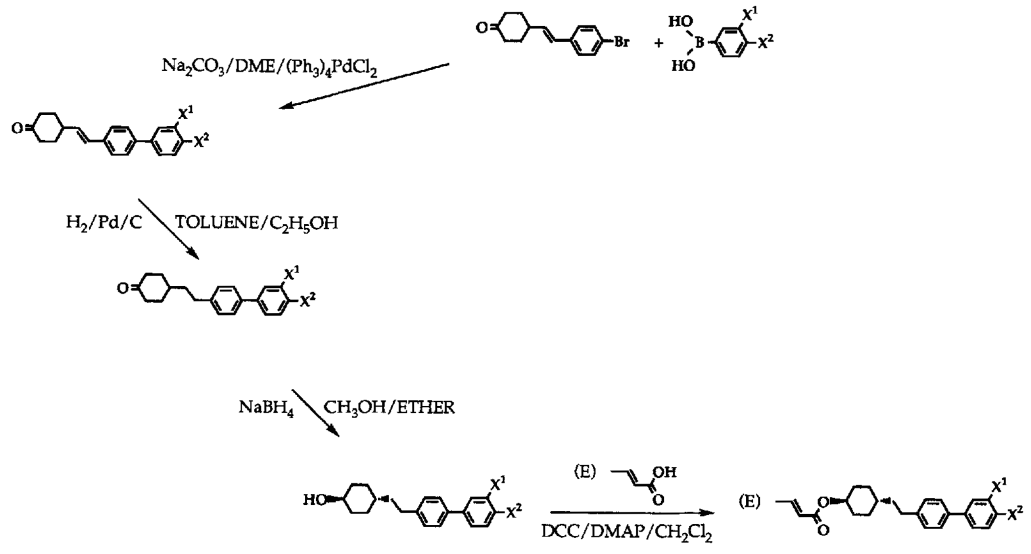

(36 and 37)

Scheme 5.

2. Synthesis

The desired *trans*-4-substituted-cyclohexyl (*E*)-alk-2-enoates were synthesized in two steps from a wide variety of 4-substituted-cyclohexanones usually synthesized previously in other programs as intermediates for alkenyl- and (*E*)-methoxypropenyl-substituted nematogens [41, 44] and prepared according to literature methods [44] where necessary. These 4-substituted-cyclohexanones were reduced using sodium borohydride to the corresponding *trans*-4-substituted-cyclohexan-1-ols, which were esterified using DCC and DMAP [60] in the usual way with commercially available (*E*)-alk-2-enoic acids (especially (*E*)-but-2-enoic acid) to yield the desired esters. The general methods of synthesis of the two- and three-ring esters (**16–21**; **22–28** and **39–42**, respectively), the biphenyl esters (**29–31**) and the two- and three-ring ethanes (**32–37**) are illustrated in the reaction schemes 1–5, respectively. The general methods of preparation, purification and analysis of structure and purity are described in detail in the Experimental for a typical example of the (*E*)-2-alkenoates reported here. The synthesis of the ethers (**2–5** and **13**) will be reported elsewhere [39].

3. Mesomorphic properties

The two-ring *trans*-4-substituted-phenylcyclohexyl (*E*)-but-2-enoates (**16–21**) incorporating standard end-groups (F, Cl, OCF$_3$, CN) and one lateral substituent (F) exhibit high melting points (104°C, on average) and are not in general mesomorphic, see table 2. Only the nitrile (**16**) possesses a (monotropic) nematic phase above room temperature. The melting points and enthalpies of fusion (ΔH) are unusually high for two-ring components of this kind.

The introduction of an additional *trans*-1,4-disubstituted cyclohexane ring into the (*E*)-but-2-enoates (**16–21**) to yield the three-ring (*E*)-but -2-enoates (**22–28**) results in an increase in the melting point (+ 18°C, on average, comparing only the esters with the same substituents), see table 3. No smectic phases could be observed despite substantial supercooling below the melting point. The (*E*)-but-2-enoates (**22–28**) exhibit wide-range nematic phases with high clearing points (231°C, on average). The nitrile possesses the highest clearing point, despite the presence of a fluorine atom in an *ortho*-position. The clearing point increases with increasing dipole moment of the terminal substituent, as usually observed. The introduction of a second substituent (i.e., fluorine) into the mono-substituted esters (**22** and **23**) to produce the disubstituted esters (**26** and **27**) results in a decrease in the clearing point (20°C, on average).

The replacement of the central *trans*-1,4-disubstituted cyclohexane ring of the fluoro-substituted (*E*)-but-2-enoates (**22** and **26**) to give the corresponding biphenyl esters (**29** and **31**) leads to an increase in the melting point (+ 14°C, on average) and a decrease in the clearing point (− 10°C, on average), see table 4. Thus, the nematic range is narrower (− 24°C, on average) for the biphenyls (**29** and **31**).

The introduction of an ethyl linkage into the (*E*)-but-2-enoates (**16–21**) to yield the (*E*)-but-2-enoates (**32–35**) (see table 5) results in a decrease in the melting point (− 27°C, on average). However, three of the four ethyl substituted compounds exhibit a nematic phase at elevated temperatures for two-ring materials of this type. The

Table 2. Transition temperatures and some enthalpies of fusion for the esters below.

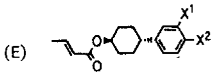

Ester	X^1	X^2	C–I/°C	N–I/°C	ΔH/kJ mol^{-1}
17	H	F	81	—	25·1
18	H	Cl	113	—	30·2
19	H	Br	115	—	28·4
20	H	OCF_3	67	—	21·6
21	F	CN	120	—	21·1
16	H	CN	128	(119)	30·3

( ) Represents a monotropic transition temperature.

Table 3. Transition temperatures and some enthalpies of fusion for the esters below.

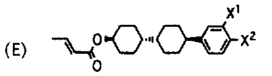

Ester	X^1	X^2	C–N/°C	N–I/°C	$\Delta T_{N\text{–}I}$/°C	ΔH/kJ mol^{-1}
22	H	F	105	219	114	27·0
23	H	Cl	129	257	128	25·8
24	H	CF_3	157	199	42	15·8
25	H	OCF_3	83	229	146	22·2
26	F	F	103	201	98	25·1
27	F	Cl	134	233	99	26·9
28	F	CN	137	280	143	22·8

Table 4. Transition temperatures and some enthalpies of fusion for the esters below.

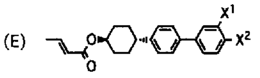

Ester	X^1	X^2	C–N/°C	N–I/°C	$\Delta T_{N\text{–}I}$/°C	ΔH/kJ mol^{-1}
29	H	F	122	216	94	21·5
30	H	CN	171	290	120	27·2
31	F	F	113	184	71	29·7

Table 5. Transition temperatures and some enthalpies of fusion for the esters below.

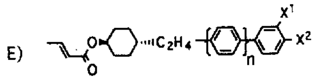

Ester	n	X^1	X^2	C–N/I/°C	N–I/°C	$\Delta T_{N\text{–}I}$/°C	ΔH/kJ mol^{-1}
32	0	H	F	62	—	—	25·0
33	0	H	Cl	73	(44)	—	
34	0	H	Br	89	(43)	—	28·6
35	0	H	CN	96	(91)	—	
36	1	F	F	105	138	33	33·3
37	1	F	Cl	92	167	75	22·7

( ) Represents a monotropic transition temperature.

Table 6. Transition temperatures and some enthalpies of fusion for the esters below.

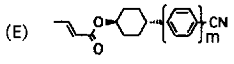

Ester	m	C–N/I/°C	N–I/°C	$\Delta T_{N\text{–}I}$/°C	ΔH/kJ mol^{-1}
38	0	93	—	—	24·4
16	1	128	(119)	—	30·3
30	2	171	290	120	

( ) Represents a monotropic transition temperature.

Table 7. Transition temperatures and some enthalpies of fusion for the esters below.

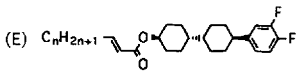

Ester	n	C–N/°C	N–I/°C	$\Delta T_{N\text{–}I}$/°C	ΔH/kJ mol^{-1}
26	1	103	201	98	25·1
39	2	80	163	83	
40	3	93	161	68	
41	4	59	141	82	
42	5	73	144	71	

Table 8. Transition temperatures for the compounds below.

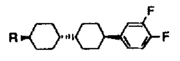

Compound	R	C–N/°C	N–I/°C	$\Delta T_{N\text{–}I}$/°C
43		47	127	80
44	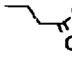	60	136	76
45	(E) 	45	145	100
26	(E) 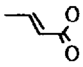	103	201	98

melting and clearing points of ethyl-substituted nitrile (**35**) are both lower (− 32°C and − 28°C) than those of the corresponding nitrile with a covalent bond between the rings. This may well be due to the added flexibility of the ethyl linkage and the reduced length/breadth ratio due to the displacement of the two cyclohexane rings from a common collinear axis.

The biphenyls (**36** and **37**) with one 1,4-disubstituted benzene ring more than the corresponding two-ring ethyl-substituted (*E*)-but-2-enoates (**32**–**35**) results in higher melting points, but also much higher clearing points, although a direct comparison is not possible due to the presence of different substituents. The nematic range

Table 9. Structures, transition temperatures and codes for the reference substance (3CPOd$_3$1) and fluorinated bicyclohexanes with (*E*)-methoxypropenyl, methoxypropyl, (*E*)-propenyl and (*E*)-but-2-enoyloxy terminal groups.

Code		Compound	C–S/N/°C	S–N/°C	N–I/°C
3CPOd$_3$1	(E)	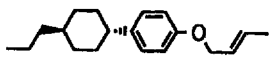	42	—	58
101d$_1$CCP$_F$F	(E)	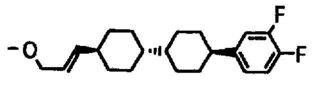	47	—	133
103CCP$_F$F		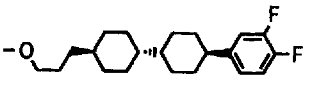	48	(42)	130
1d$_1$CCP$_F$F	(E)	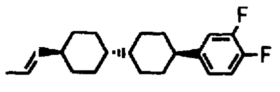	49	65	159
1d$_3$ECCP$_F$F	(E)	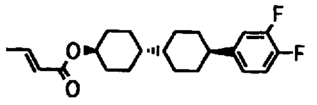	103	—	201

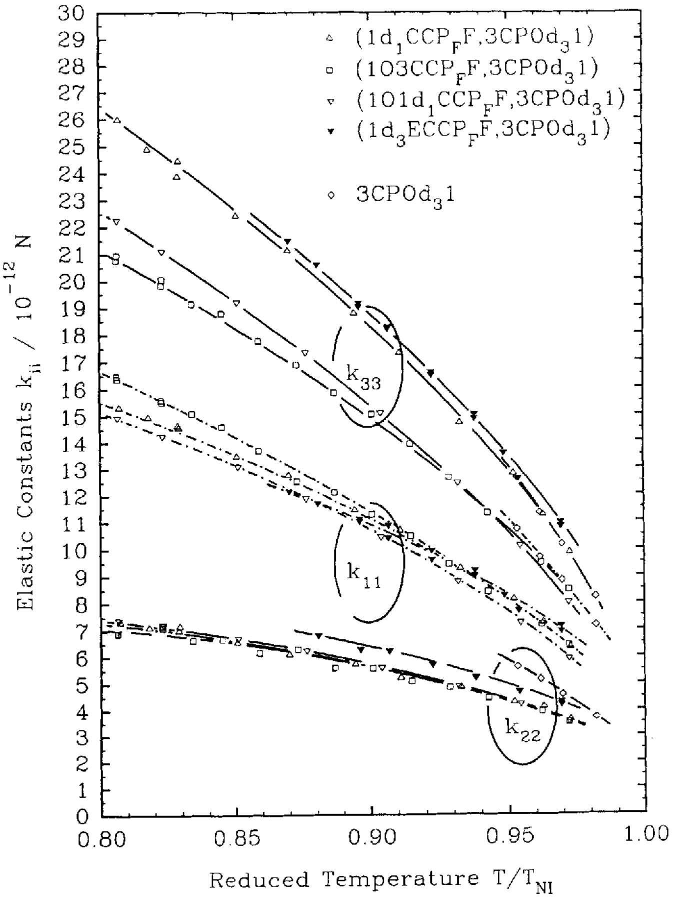

Figure 1. Plots of the elastic constants k_{ii} against reduced temperature T/T_{NI} for the pure compound 3CPOd$_3$1 and the binary mixtures 1d$_1$CCP$_F$F/3CPOd$_3$1, 103CCP$_F$F/3CPOd$_3$1, 101d$_1$CCP$_F$F/3CPOd$_3$1 and 1d$_3$ECCP$_F$F/3CPOd$_3$1.

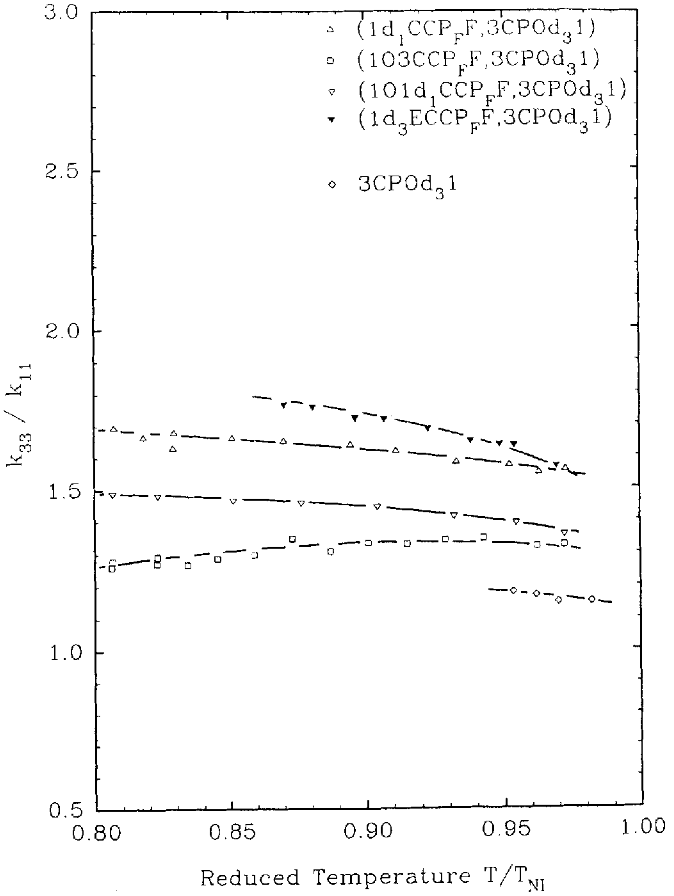

Figure 2. Plots of the elastic constant ratio k_{33}/k_{11} against reduced temperature T/T_{NI} for the pure compound 3CPOd$_3$1 and the binary mixtures 1d$_1$CCP$_F$F/3CPOd$_3$1, 103CCP$_F$F/3CPOd$_3$1, 101d$_1$CCP$_F$F/3CPOd$_3$1 and 1d$_3$ECCP$_F$F/3CPOd$_3$1.

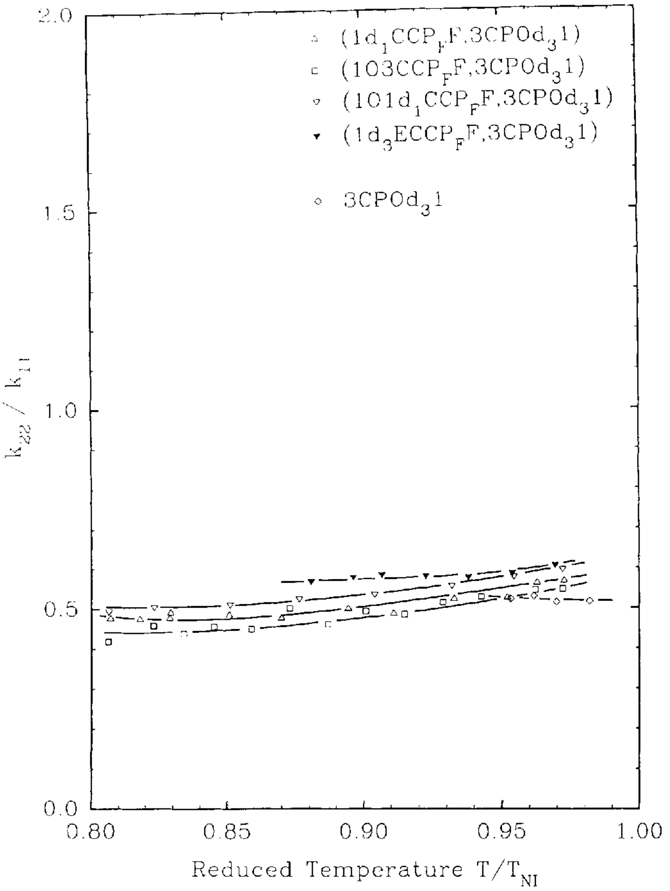

Figure 3. Plots of the elastic constant ratio k_{22}/k_{11} against reduced temperature T/T_{NI} for the pure compound $3CPOd_31$ and the binary mixtures $1d_1CCP_FF/3CPOd_31$, $103CCP_FF/3CPOd_31$, $101d_1CCP_FF/3CPOd_31$ and $1d_3ECCP_Ff/3CPOd_31$.

is much broader. Comparisons with the analogous biphenyls (**29** and **31**) with direct bonds between the cyclohexyl and phenyl rings reveal lower melting points (− 20°C, on average) and clearing points (− 48°C, on average) for the ethyl-substituted esters. The same arguments as above can be used to rationalize these effects.

It is clear from the data collated in table 6 that at least two rings are required for mesophase formation, despite the high nematic tendencies of the benzonitriles incorporating the (*E*)-but-2-enoyloxy moiety. The one-ring cyclohexane (**38**) is not mesomorphic despite an anticipated degree of interdigitation/dimer formation. The two-ring benzonitrile (**16**) exhibits a monotropic nematic phase at a high temperature for a two-ring compound. The clearing point of the three-ring benzonitrile (**30**) is very high and the width of the nematic phase is large.

The transition temperatures for a short homologous series of *trans*-4(*trans*-4-[3,4-difluorophenyl]cyclohexyl)cyclohexyl (*E*)-alk-2-enoates (**26** and **39**–**42**) are collated in table 7. The relatively low melting points and high clearing points result in relatively wide nematic phases. No smectic phases could be observed despite a degree of supercooling below the melting point. Both the melting and clearing points decrease with increasing chain length. A degree of alternation in the clearing point is observed.

The effect of systematically introducing oxygen atoms (O) and double bonds (C=O and C=C) into the 1-*trans*-4-(*trans*-4-pentylcyclohexyl)cyclohexyl-3,4-difluorobenzene (**43**) to yield the 1-*trans*-4-*trans*-4-[(*E*)-but-2-enoyloxy]cyclohexyl)cyclohexyl-3,4-difluorobenzene (**26**) is demonstrated in table 8. Increasing the polarity of the chain by introducing a carboxy group (CO_2) to produce the ester (**44**) does not change the width of the nematic phase significantly, as both the melting and the clearing point are increased by similar amounts (+ 13°C and + 9°C). The added stiffness induced by the introduction of a carbon–carbon double bond into the chain increases the clearing point substantially (+ 18°C) while decreasing the melting point slightly (− 2°C) for the compound (**45**) [41]. The combination of all these elements to produce the (*E*)-but-2-enoate (**26**) yields the highest melting and clearing point and an equally wide nematic phase. No conjugation between the ester group and the cyclohexane ring is possible.

4. Mixture properties

Selected physical properties of four binary mixtures M1–4 of a weakly polar standard nematic liquid crystal [(*E*)-3-pentenyl 4-(*trans*-4-propylcyclohexyl)phenyl ether [41] (code: $3CPOd_31$)] and four difluoro-substituted (polar) bicyclohexanes have been evaluated and compared, see tables 9–11 and figures 1–7. The four difluoro-substituted liquid crystals incorporate the (*E*)-methoxypropenyl (code: $101d_1CCP_FF$ [42–44]), the methoxypropyl (code: $103CCP_FF$) [32], the 1-(*E*)-propenyl (code: $1d_1CCPF$) [41] and the (*E*)-but-2-enoyloxy (**26**; code: $1d_3ECCP_FF$) terminal groups, see table 9. Two of the comparison compounds $103CCP_FF$ and $1d_1CCP_FF$ are important components of (commercially available) nematic mixtures for LCDs and the third ($101d_1CCP_FF$) has been recently reported [42–44] as a promising candidate for LCD applications. However, binary mixtures (50:50 mol%) are required so that the physical properties of interest can be measured at temperatures ($T < 80$°C) within the operating range of standard instruments. Due to the high T_{NI} of the ester ($1d_3ECCP_FF$), some of the data recorded in tables 10 and 11 were extrapolated from higher temperature data taken from the plots in figures 1–7. Representative data at two temperatures $T_{NI} - 10$°C and $T_{NI} \times 0{\cdot}8$) for the four binary mixtures (M1–4) under investigation are collated in tables 10 and 11.

Table 10. Elastic, dielectric and optical properties of (1 : 1 mol %) binary mixtures M1–4 of the reference compounnd ($3CPOd_31$) with the compounds $101d_1CCP_FF$, $103CCP_FF$, $1d_1CCP_FF$ and $1d_3ECCP_FF$. The data in italics were determined at (T_{NI} − 10°C). The others were measured at 0·8 × T_{NI}.

Liquid crystal	$\kappa_{11}/$ 10^{-12}N	$\kappa_{22}/$ 10^{-12}N	$\kappa_{33}/$ 10 − 12 N	k_{33}/k_{11}	$\kappa/$ 10^{-12}N	$\varepsilon_\perp$	$\Delta\varepsilon$	$\Delta\varepsilon/\varepsilon_\perp$	n_0	Δn
$3CPOd_31$	8·82	4·55	10·14	1·16	9·1	3·07	− 0·27	− 0·09	1·486	0·089
M1 = ($101d_1CCP_FF/3CPOd_31$)(1 : 1)	*5·90*	*3·50*	*8·00*	*1·36*	*6·2*	*3·88*	*1·34*	*0·35*	*1·477*	*0·073*
	15·20	7·50	22·75	1·50	17·1	4·25	2·57	0·60	1·432	0·107
M2 = ($103CCP_FF/3CPOd_31$)(1 : 1)	*6·33*	*3·60*	*9·86*	*1·56*	*7·0*	*3·44*	*1·84*	*0·53*	*1·474*	*0·076*
	15·60	7·40	26·45	1·70	18·5	3·53	3·27	0·33	1·490	0·099
M3 = $1d_1CCP_FF/3CPOd_31$)(1 : 1)	*6·33*	*3·60*	*9·86*	*1·86*	*7·0*	*3·44*	*1·84*	*0·53*	*1·474*	*0·076*
	15·60	7·40	26·45	1·70	18·5	3·53	3·27	0·33	1·490	0·109
M4 = ($1d_3ECCP_FF/3CPOd_31$)(1 : 1)	*6·65*	*4·05*	*10·25*	*1·54*	*7·2*	*4·34*	*1·51*	*0·35*	*1·468*	*0·079*
	14·6†	8·3†	26·8†	1·84†	17·2†	—	—	—	1·483	0·115

†Extrapolated values.

The four binary mixtures M1–4 exhibit broadly similar plots of the elastic constants ($k_{ii} = k_{33}$, k_{22} and k_{11}; splay, twist and bend, respectively) against reduced temperature (T/T_{NI}), see figure 1. It is, therefore, not surprising that the plots of the ratios (k_{33}/k_{11} and k_{22}/k_{11} against T/T_{NI} for the binary mixtures are also similar, see figures 2 and 3. The values of the elastic constants k_{33} and k_{22} are highest and k_{11} the lowest for mixtures containing the ester (**26**; code: $1d_3ECCP_FF$), see table 10. This non-linear behaviour could be used to obtain steep voltage-transmission characteristics in supertwisted nematic displays (STN-LCDs), where high values of k_{33}/k_{11} are required [40].

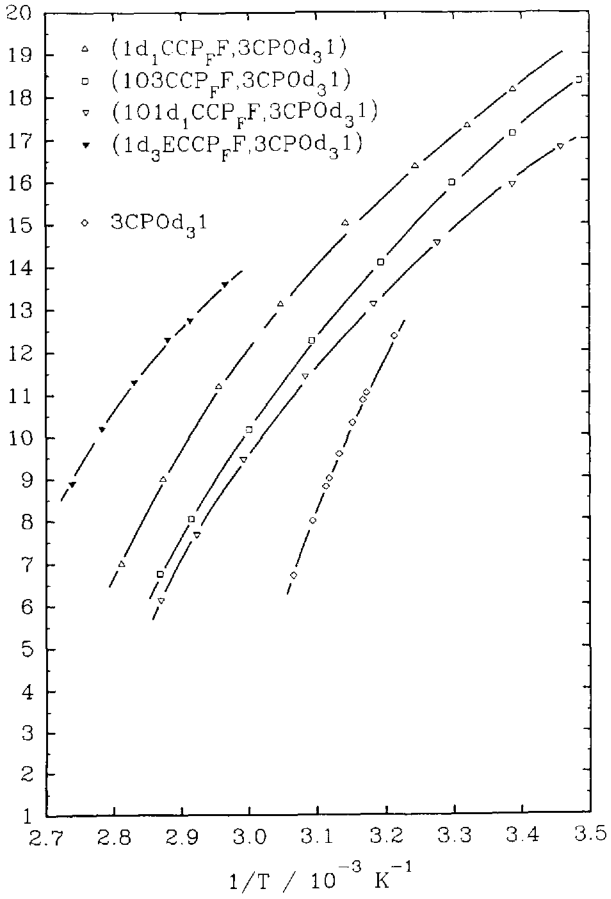

Figure 4. Plots of the elastic expression $\kappa = k_{11} + (k_{33} - 2k_{22})/4$ against the temperature reciprocal for the pure compound $3CPOd_31$ and the binary mixtures $1d_1CCP_FF/3CPOd_31$, $103CCP_FF/3CPOd_31$, $101d_1CCP_FF/3CPOd_31$ and $1d_3ECCP_FF/3CPOd_31$.

The plots and absolute values of the elastic expression $\kappa = k_{11} + (k_{33} - 2k_{22})/4$ against T/T_{NI} for the four binary mixtures M1–4 are similar, see figure 4 and table 10. The elastic expression κ and the dielectric anisotropy ($\Delta\varepsilon = \varepsilon_\parallel - \varepsilon_\perp$) determine the threshold voltage of twisted nematic TN-LCDs ($V_{10} \propto V_c = \pi(\kappa/\varepsilon_0\Delta\varepsilon)^{1/2}$) [1]. The dielectric anisotropy of the mixture M4 containing the ester $1d_3ECCP_FF$ is the second lowest for the four mixtures, see table 11. This indicates a lateral contribution from the ester (carboxy) group, as is seen in the value for $\varepsilon_\perp$. This combination of κ and $\Delta\varepsilon$ results in the highest threshold voltage for the four mixtures under investigation, see table 11.

The plot of the rotational viscosity γ_1 against $1/T$ of the binary mixture M4 containing the ester $1d_3ECCP_FF$, as shown in figure 5, lies clearly higher than those of the other binary mixtures M1–M3, see also table 10. This is not surprising, as esters normally exhibit higher viscosity values than alkanes or ethers. Comparisons of viscosity and viscoelastic ratios should be made at constant temperatures (for example, 22°C). However, although this is not possible in this case due to crystallization problems close to room temperature, the general trends observed at higher (reduced) temperatures are certainly indicative of the behaviour at room temperature.

The plots of the visco-elastic ratio γ_1/κ of all the binary mixtures are very similar in shape, see figure 6. The values for the binary mixture M4, containing the ester $1d_3ECCP_FF$, lie somewhat higher than those of the other binary mixtures M1–M3, see also table 11. The ratio γ_1/κ

Table 11. Rotational viscosity, visco-elastic ratio, response times t_{on} and t_{off} and TN-LCD threshold voltage V_{10} at 10 per cent transition of (1 : 1 mol %) binary mixtures M1–4 of the reference compound (3CPOd$_3$1) with the compounds 101d$_1$CCP$_F$F, 103CCP$_F$F, 1d$_1$CCP$_F$F and 1d$_3$ECCP$_F$F. The data in italics were determined at (T_{NI} − 10°C). The others were measured at 0·8 × T_{NI}.

Liquid crystal	γ_1/cP	$\gamma_1/\kappa/^{-1}10^{-12}\,m^{-2}\,s^{-1}$	t_{on}/ms	t_{off}/*ms*	V_{10}/V
3CPOd$_3$1	*25*	*2·7*			
	86				
M1 = (101d$_1$CCP$_F$F/3CPOd1)(1 : 1)	*16·4*	*2·6*	*6*	*12*	*2·47*
	260	15·2	24	42	3·38
M2 = (103CCP$_F$F/3CPOd$_3$1)(1 : 1)	*14·8*	*2·2*	*5*	*11*	*2·01*
	225	12·2	20	41	2·76
M3 = (1d$_1$CCP$_F$F/3CPOd$_3$1)(1 : 1)	*10·9*	*1·6*	*3*	*6*	*2·32*
	140	7·6	13	21	3·18
M4 = (1d$_3$ECCP$_F$F/3CPOd$_3$(1 : 1)	*13·6*	*1·9*	*4·1*	*8·1*	*2·59*
	215	12·5	15·6	24·3	3·62

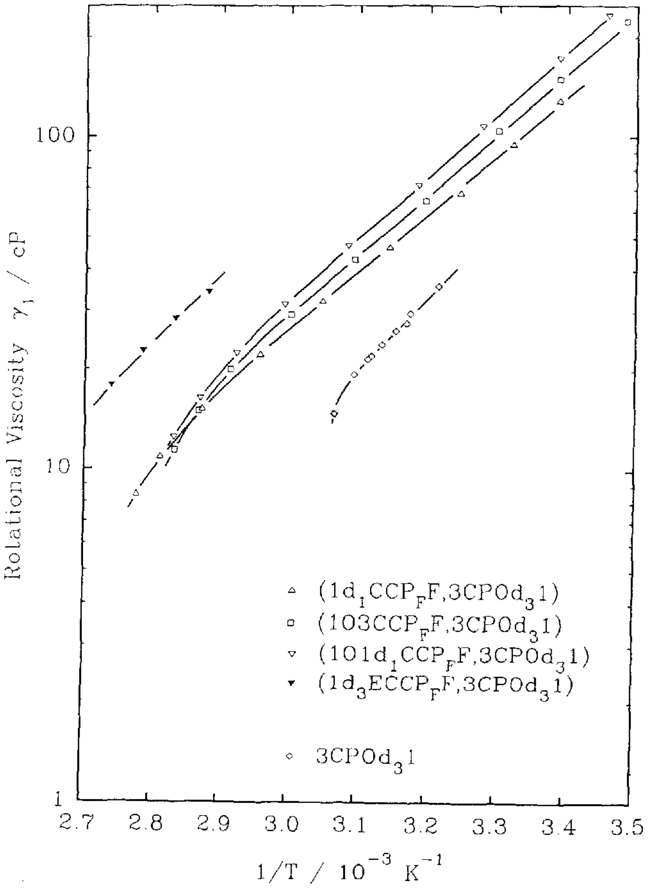

Figure 5. Plots of the rotational viscosity γ_1 against the temperature reciprocal for the pure compound 3CPOd$_3$1 and the binary mixtures 1d$_1$CCP$_F$F/3CPOd$_3$1, 103CCP$_F$F/3CPOd$_3$1, 101d$_1$CCP$_F$F/3CPOd$_3$1 and 1d$_3$ECCP$_F$F/3CPOd$_3$1.

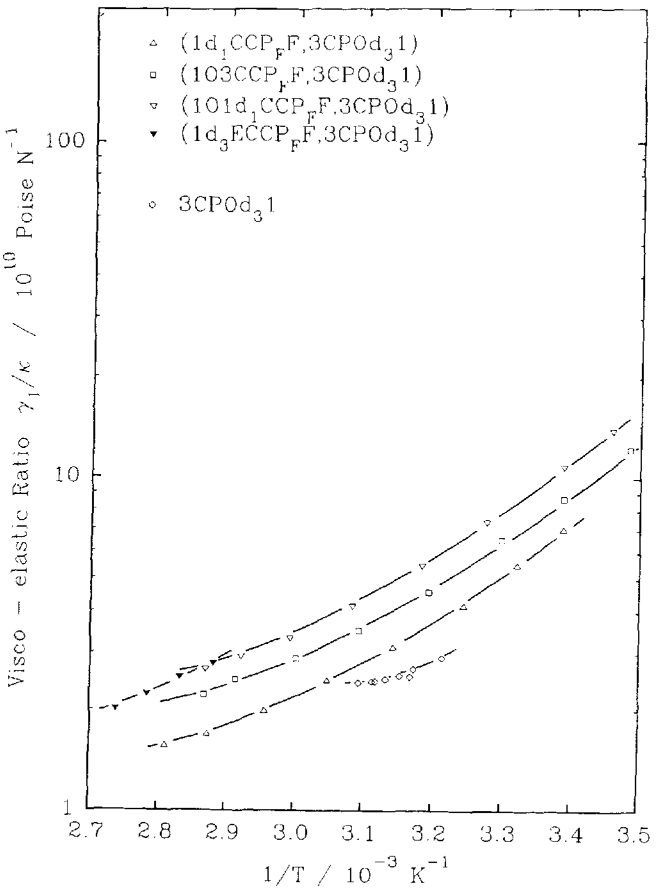

Figure 6. Plots of the viscoelastic ratio γ_1/κ against the temperature reciprocal for the pure compound 3CPOd$_3$1 and the binary mixtures 1d$_1$CCP$_F$F/3CPOd$_3$1, 103CCP$_F$F/3CPOd$_3$1, 101d$_1$CCP$_F$F/3CPOd$_3$1 and 1d$_3$ECCP$_F$F/3CPOd$_3$1.

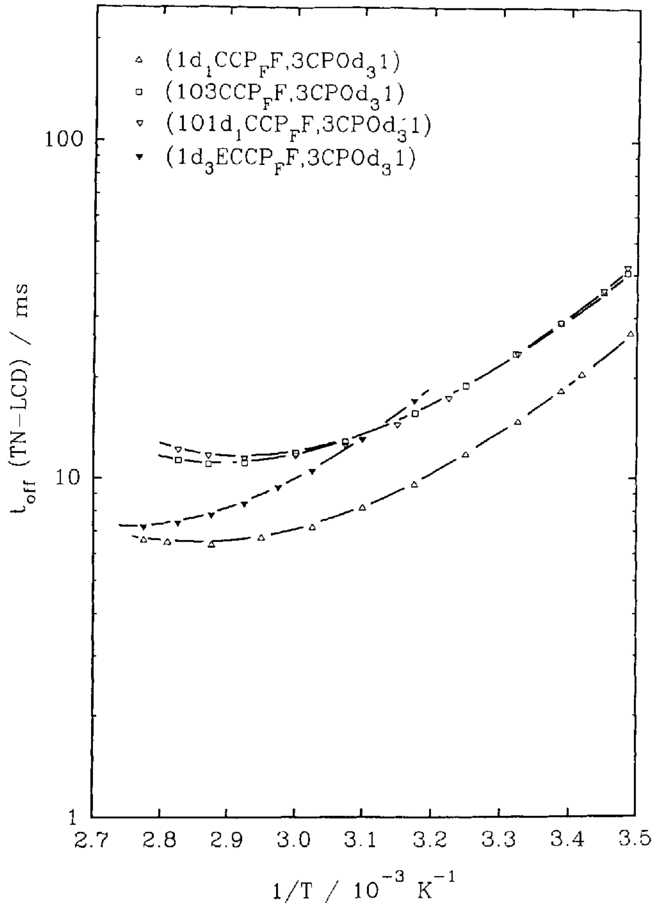

Figure 7. Plots of the switch off times T_{off} against the temperature reciprocal for the binary mixtures 1d$_1$CCP$_F$F/3CPOd$_3$1, 103CCP$_F$F/3CPOd$_3$1, 101d$_1$CCP$_F$F/3CPOd$_3$1 and 1d$_3$ECCP$_F$F/3CPOd$_3$1.

basically determines the switch off times $t_{\mathrm{off}} \propto \gamma_1/\kappa$ in TN-LCDs cells [40]. The ratio γ_1/κ and thus t_{off} are similar for the two binary mixtures M1 and M2 containing the compounds 101d$_1$CCP$_F$F and 103CCP$_F$F with oxygen in the chain, see figures 6 and 7 and table 11. The response times of the mixture M3 incorporating the (*E*)-propenyl-substituted compound (1d$_1$CCP$_F$F) are shorter due to the shorter chain. However, the surprisingly low value for the mixture M4 containing the (*E*)-but-2-enoyloxy-substituted material (1d$_3$ECCP$_F$F) cannot be explained in this way, see figure 7 and table 11.

Of the four binary mixtures M1–4 under study, the birefringence (Δn) is highest for the mixture M4 containing the (*E*)-but-2-enoyloxy-substituted material (1d$_3$ECCP$_F$F), see table 10. This is probably due to the combination of the carboxy (CO_2) group and the double bond.

The results of photochemical and thermal stability tests for the standard, moderately polar ($\Delta\varepsilon = +3{\cdot}99$) nematic mixture (M5; 100 wt %) and for binary mixtures of the ester (**26**; code: 1d$_3$ECCP$_F$F; 15 wt %) and the standard mixture (M5; 85 wt %) are collated in tables 12 and 13. The dielectric anisotropy and T_{NI} of the ester mixture are higher due to the high values for the pure ester. The resistivity (Ωm, 25°C) and holding ratios (180°C) [61] for both mixtures before irradiation with ultraviolet (UV) light (Hanau Suntest) (0 h) are comparable. After the test time (110 H), the resistivity values and the holding ratios are still comparable. A series of heating tests were carried out on three mixtures of identical initial composition, i.e. for 72 h at 100°C in a closed ampoule, at 180°C for 1 h in a closed ampoule and at 150°C for 1 h in an open ampoule. Although the values for the resistivity of the ester mixtures at the start of the experiments are slightly lower, no significant change is observed in the resistivity of any of the mixtures during the heating tests. No decrease in the clearing point of the ester mixture could be determined.

Thus, the new (*E*)-alk-2-enoates show broadly comparable physical properties and electro-optical characteristics to those of some analogous components of commercially available nematic mixtures for LCDs. However, the broad nematic phases, absence of smectic phases, high clearing points, the high thermal and photochemical stability, large k_{33}/k_{22} values and surprisingly moderate viscosity of some of the new (*E*)-alk-2-enoates are attractive properties for the design of nematic mixtures of positive dielectric anisotropy.

5. Experimental

The configuration of the carbon–carbon double bond in the alkenyl chain of the new esters (**16–42**) was confirmed by ^{1}H NMR spectroscopy (the *trans*-olefinic coupling constants ≈ **12–18** Hz are larger than those of the corresponding *cis*-olefinic coupling constants ≈ 7–11 Hz) and by infrared spectroscopy (the *trans*-absorption bands are narrow and exact ≈ 970–960 cm^{-1}, while the *cis*-absorption bands are observed at distinctly different wavelengths ≈ 730–675 cm^{-1}). The structural and isomeric purity was determined by thin layer chromatography (TLC) and gas chromatography (GC) as usual (where necessary, on liquid crystal packed columns [62]) and by differential thermal analysis (DTA). A Perkin–Elmer 8310 capillary gas chromatograph and GP-100 graphics printer and a Mettler DTA TA 2000 were used. 4 cm × 8 cm precoated TLC plates, SiO_2 SIL G/UV$_{254}$, layer thickness 0·25 mm (Machery-Nagel, Düren, Germany) were utilized. A small amount (0·2 per cent) of the but-3-enoyloxy isomer was found to be present in all of the (*E*)-but-2-enoyloxy-substituted esters. Isomerization was found to occur on GC columns at high temperatures.

The transition temperatures of the esters prepared and recorded in tables 1–9 were determined by optical microscopy using a Leitz Ortholux II POL BK microscope

Table 12. Resistivity and holding ratio for the base mixture M5 (100 wt %) and the mixture M6 containing the ester 1d$_3$ECCPF$_F$ (15 wt %) and the base mixture M5 (85 wt %) in a Hanau Suntest apparatus.

Resistivity/Ωm (25°C)	Mixture M5 (100 wt %)	Mixture M6 1d$_3$ECCPF$_F$ (15 wt %)/M5(85 wt %)
ρ (display) $t = 0$ h UV	6·1 e^{11}	1·5 e^{11}
Holding ratio (80°C)	99·6	99·0
ρ (display $t = 110$ h UV	3·1 e^{10}	2·2 e^{10}
Holding ratio (80°C)	95·6	92·9

Table 13. Resistivity, dielectric properties and the clearing point for the base mixture M5 (100 wt %) and the mixture M6 containing the ester 1d$_3$ECCPF$_F$ (15 wt %) and the base mixture M5 (85 wt %) in ampoules (closed or open) in an oven.

Resistivity/Ωm (25°C)	Mixture M5 (100 wt %)	Mixture M6 1d$_3$ECCPF$_F$ (15 wt %)/M5 (85 wt %)
ρ (bulk) $t = 0$ h	1·1 e^{12}	9·3 e^{11}
ρ (bulk) $t = 72$ H, 100°C (cl)	1·1 e^{12}	5·4 e^{11}
ρ(bulk) $t = 1$ h, 180°C (cl)	1·2 e^{11}	5·4 e^{10}
ρ(bulk) $t = 1$ h, 150°C (op)	8·2 e^{10}	9·7 e^{10}
Dielectric anisotropy $\Delta\varepsilon$	3·99	4·45
Dielectric permitivity $\langle\varepsilon\rangle$	4·93	5·43
Clearing point °C	107·4	118·2

(cl) = closed ampoules.
(op) = open ampoules.

in conjunction with a Mettler FP82 heating stage and FP80 control unit. All the monotropic liquid crystal phases could be observed directly. The Mettler stage could be cooled (− 50°C) by allowing N$_2$ gas, cooled by liquid N$_2$, to pass through the stage at a controlled rate. The transition temperatures were also determined using a Mettler DTA TA 2000.

Column chromatography was carried out using silica gel 60 (230–400 mesh ASTM). Reaction solvents and liquid reagents were purified by distillation or drying shortly before use. Reactions were carried out under N$_2$, unless water was present as a reagent or solvent. All temperatures were measured externally unless otherwise stated. The ^{1}H-NMR spectra were recorded at 60 MHz/Varian T-60, 80 MHz (Bruker WP-80) or 270 MHz (Bruker HX-270) Mass spectra were recorded on an MS9 (AEZ Manchester) spectrometer.

The determination of the physical properties of the nematic mixtures containing the new esters was carried out as previously described [63–64]. The mixture M5 consists of 1,2-difluoro-4-[*trans*-4-(*trans*-4-[(*E*)-1-propenyl]cyclohexyl)cyclohexyl]benzene (34·0 wt %), 1,2-difluoro-4-[*trans*-4-(*trans*-4-[ethenyl]-cyclohexyl)cyclohexyl]benzene (34·0 wt %) and (28·0 wt %) of the mixture 8486 [composition: ethyl *trans*-4-(*trans*-4-[3-butenyl]cyclohexyl)cyclohexyl ether (25·0 wt %), methyl *trans*-4-(*trans*-4-[(*E*)-3-pentenyl]cyclohexy)cyclohexyl ether (13·0 wt %), methyl [*trans*-4-(*trans*-4-[(*E*)-1-propenyl]cyclohexyl)-cyclohexyl]methyl ether (10·0 wt %), ethyl 4-(2-[*trans*-4-(pentylcyclohexyl)]ethyl)phenyl ether (30·0 wt %), 1-methyl-4-[*trans*-4-(*trans*-4-[(*E*)-1-propenyl]cyclohexyl)cyclohexyl]benzene (9·0 wt %), and *trans*-1-butyl-4-[2-(4-[2-(4-[*trans*-4-(pentylcyclohexyl)]phenyl)ethyl]cyclohexane (13·0 wt.%)].

5.1. *trans-4-(trans-4-Trifluoromethoxyphenyl]cyclohexyl (E)-but-2-enoate* (**25**)

A solution of *N,N*-dicyclohexylcarbodiimide (0·66 g, 3·2 mmol) in dichloromethane (50 cm^3) was added slowly to a solution of *trans*-4-(*trans*-4-[4-trifluoromethoxyphenyl]cyclohexyl)cyclohexan-1-ol (0·55 g, 1·6 mmol), (*E*)-but-2-enoic (crotonic) acid (Fluka) (0·28 g, 3·2 mmol), 4-dimethylamino)pyridine (0·04 g) and dichloromethane (25 cm^3) cooled in an ice bath under an atmosphere of nitrogen. After filtration to remove precipitated material, the filtrate was evaporated down under reduced pressure. The residue was purified by column chromatography on silica gel using a 9:1 hexane/ethyl acetate mixture as eluent, followed by recrystallization from ethanol to yield the pure ester (yield 0·21 g, 35 per cent). ^{1}H NMR (CDCl$_3$): 1·15–1·89 (21 H, overlapping peaks), 2·50 (1 H, overlapping peaks), 5·82–5·88 (1H, d), 6·82–6·85 (2 H, overlapping peaks), 7·13–7·26 (2 H, d), 7·02–7·14 (2 H, d). ν_{max}: 2918, 2856, 1709, 1652, 1509, 1267, 1219, 1194, 1018, 978, 840 cm^{-1}. *m/z*: 410 (M^+, 324 ($C_{19}H_{23}O$) 188 ($C_9H_7F_3O$). The transition temperatures of this ester (**25**) and similar esters (**16–24** and **26–42**) prepared using this general method are collated in tables 1–8.

5.2. *trans-4-(trans-4-[4-Trifluoromethoxyphenyl]cyclohexyl)cyclohexan-1-ol*

A solution of *trans*-4-(*trans*-4-[4-trifluoromethoxyphenyl]cyclohexyl)cyclohexanone (0·86 g, 2·5 mmol) and a mixture of 9 : 1 methanol/ether (30 cm^3) was added dropwise to a freshly prepared mixture of sodium borohydride (0·2 g, 5·2 mmol) and a mixture of 9 : 1 methanol/ether (25 cm^3) at 0°C. After the addition was complete, the reaction mixture was stirred overnight at room temperature. A 25 per cent hydrochloric acid solution was added carefully to the reaction mixture, which was shaken with ethyl acetate ($3 \times 50\,cm^3$). The combined organic extracts were washed with water (2×500 ml) and dilute sodium carbonate solution (2×500 ml), dried ($MgSO_4$), filtered and then evaporated down. The residue was purified by column chromatography on silica gel using a 7 : 3 hexane/ethyl acetate mixture as eluent and recrystallization from ethanol to yield the pure alcohol (0·6 g, 70 per cent). ^1H NMR ($CDCl_3$): 1·15 (12 H, overlapping peaks), 1·56 (8 H, overlapping peaks), 2·49–2·50 (1 H, t), 3·50 (1 H, s), 7·13–7·19 (2 H, d), 7·22–7·26 (2 H, d). IR (KBr)ν_{max}: 3374, 2927, 2855, 1508, 1454, 1270, 1225, 1155, 1058, 825 cm^{-1}. MS *m/z*: 342 (M^+), 324 ($C_{19}H_{23}F_3O_2$), 188($C_9H_7F_3O$), 175($C_8H_6F_3O$).

The authors express their gratitude to Mr B. Blöchliger, Mr C. Haby, Mrs V. Kannookadan and Mr Hp. Mohn for technical assistance in the preparation and evaluation of the compounds. Dr W. Arnold (NMR), Mr W. Meister (MS), Dr M. Grosjean (IR), Mr F. Wild and Mr B. Halm (DTA) are thanked for the measurement and interpretation of the required spectra.

References

[1] Schadt, M., and Helfrich, W., 1971, *Appl. Phys., Lett.*, **18,** 127.
[2] Howard, W. E., 1986, *Proc. SID, '86*, p. 313.
[3] Morozumi, S., Ohta, T., Araki, R., Kubota, K., Ono, Y., Nakazawa, T., and Ohara, H., 1983, *SID '84 Digest, Japan Display '83*, p. 404.
[4] Scheffer, T. J., and Nehring, J., 1984, *Appl. Phys., Lett.*, **45,** 1021.
[5] Kando, Y., Nakagomi, T., and Hawasaga, S., 1985, German Patent DE-3 503 259 Al.
[6] Schadt, M., and Leenhouts, F., 1987, *Proc. SID*, **28,** 275.
[7] Katoh, K., Endo, Y., Akatsuka, M., Ohgawara, M., and Sawada, K., 1987, *Jap. J. appl. Phys.*, **26,** L1784.
[8] Okumura, O., Nagata, M., and Wada, K., 1987, *ITEJ Tech. Rep. II*, p. 27.
[9] White, D. L., and Taylor, G. N., 1974, *J. appl. Phys.*, **45,** 4718.
[10] Waters, C., Brimmel, V., and Raynes, E. P., 1983, *Proc. Japan Display '83*, p. 396.
[11] Schadt, M., 1993, *Liq. Crystals*, **14,** 73.
[12] Demus, D., Demus, H., and Zaschke, H., 1974, *Flüssige Kristalle in Tabellen* (Deutscher Verlag für Grundstoff Industrie, Leipzig).
[13] Demus, D., and Zaschke, H., 1984, *Flüssige Kristalle in Tabellen*, Vol. II (Deutscher Verlag für Grundstoff Industrie, Leipzig).
[14] Gray, G. W., 1976, *Advances in Liquid Crystals*, Vol. 2, edited by G. H. Brown (Academic Press), p. 16 and references therein.
[15] Toyne, K., 1987, *Thermotropic Liquid Crystals*, edited by G. W., Gray (Wiley), and references therein.
[16] Coates, D., 1990, *Liquid Crystal Applications and Uses*, Vol. 1, edited by T. Bahudar (World Scientific Press), p. 91, and references therein.
[17] Gray, G. W., Harrison, K. J., and Nash, J. A., 1973, *Electronics Lett.*, **9,** 130.
[18] Deutscher, H.-J., Laaser, B., Doelling, W., and Schubert, H., 1978, *J. prakt. Chem.*, **320,** 191.
[19] Eidenschink, R., Erdmann, D., Krause, J., and Pohl, L., 1977, *Angew. Chem. Int. Ed.*, **11,** 633.
[20] Boller, A., Cereghetti, M., Schadt, M., and Scherrer, H., 1977, *Molec. Crystals*, **42,** 215.
[21] Eidenschink, R., and Roemer, M., 1983, *13. Freiburger Arbeitstagung Flüssige Kristalle.*
[22] Takatsu, H., Takeuchi, K., and Sato, H., 1984, *Molec. Crystals liq. Crystals*, **112,** 165.
[23] Kelly, S. M., and Schad, Hp., 1985, *Helv. chim. Acta*, **68,** 1444.
[24] Finkenzeller, U., Kurmeier, A., and Poetsche, E., 1989, *18. Freiburger Arbeitstagung Flüssige Kristalle.*
[25] Schadt, M., Petrzilka, M., Gerber, P., Villiger, A., and Trickes, G., 1983, *Molec. Crystals liq. Crystals*, **94,** 139.
[26] Carr, N., Gray, G., W., and McDonnell, D. G., 1983, *Molec. Crystals. liq. Crystals*, **97,** 13.
[27] Takatsu, H., Takeuchi, K., and Sato, H., 1983, *Japan Display '83*, p. 228.
[28] Kelly, S. M., 1991, *Molec. Crystals liq. Crystals*, **204,** 27.
[29] Gray, G. W., 1978, *Advances in Liquid Crystals for Applications* (BDH Special Publication, BDH, Poole), and references therein.
[30] Inoue, H., Inukai, T., Goto, Y., Sato, H., Fukui, M., and Yokohama, K., 1982, *German Patent DE-3 237 020 A1.*
[31] Osman, M., 1985, *Molec. Crystals liq. Crystals*, **131,** 353.
[32] Takatsu, H., Takeuki, K., Sasaki, M., and Ohnishi, H., 1991, *Molec. Crystals liq. Crystals*, **206,** 159.
[33] Schadt, M., and Petrzilka, M., 1985, *Proc. SID*, 117.
[34] Goodby, J. W., Leslie, T., Cladis, P. E., and Finn, P. L., 1984, *Liquid Crystals and Ordered Fluids*, Vol. 4, p. 89.
[35] Schadt, M., Petrzilka, M., Gerber, P., and Villiger, A, 1985, *Molec. Crystals liq. Crystals*, **122,** 241.
[36] Petrzilka, M., 1985, *Molec. Crystals liq. Crystals*, **131,** 109.
[37] Schadt, M., Buchecker, R., Villiger, A., Leenhouts, F., and Fromm, J., 1986, *IEEE Trans on Electron. Dev.*, **33,** 1187.
[38] Petrzilka, M., Buchecker, R., Lee-Schmiederer, S., Schadt, M., and Germann, A., 1987, *Molec. Crystals liq. Crystals*, **148,** 123.

[39] Buchecker, R., and Schadt, M., 1987, *Molec. Crystals liq. Crystals*, **149,** 359. Buchecker, R., and Schadt, M., (unpublished results).
[40] Schadt, M., Buchecker, R., and Müller, K., 1989, *Liq. Crystals*, **5,** 293.
[41] Schadt, M., Buchecker, R., and Villiger, A., 1990, *Liq. Crystals*, **7,** 519.
[42] Kelly, S. M., Germann, A., and Schadt, M., 1994, *Liq. Crystals*, **16,** 491.
[43] Kelly, S. M., and Schadt, M., 1993, *22. Freiburger Arbeitstagung Flüssige Kristalle.*
[44] Kelly, S. M., Germann, A., Buchecker, R., and Schadt, M., 1994, *Liq. Crystals,* **16,** 67.
[45] Kelly, S. M., and Funfschilling, J., 1993, *J. mater. Chem.*, **3,** 953.
[46] Vorländer, D., 1927, *Z. Phys. chem.* A, **126,** 449.
[47] Lauk, U. H., Skrabal, P., and Zollinger, H., 1985, *Helv. chim. Acta*, **68,** 1406.
[48] Kelly, S. M., 1993, *Liq. Crystals*, **14,** 675.
[49] Fünfschilling, J., Kelly, S. M., and Villiger, A., 1993, *Liq. Crystals*, **14,** 713.
[50] Kelly, S. M., Funfschilling, J., and Villiger, A., 1993, *Liq. Crystals*, **14,** 1169.
[51] Kelly, S. M., Fünfschilling, J., and Villiger, A., 1994, *Liq. Crystals*, **16,** 813.
[52] Maier, W., and Saupe, A., 1959, *Z. naturf.* (*a*), **14,** 882: 1960, *Ibid.*, **15,** 882.
[53] Flory, P. J., and Ronca, G., 1979, *Molec. Crystals liq. Crystals*, **54,** 311.
[54] Warner, M., 1987, *Molec. Crystals liq. Crystals*, **80,** 79.
[55] Alben, R., 1971, *Molec. Crystals liq. Crystals*, **13,** 193.
[56] Cotter, M. A., 1983, *Molec. Crystals liq. Crystals*, **97,** 29.
[57] Cotter, M. A., 1983, *Phil. Trans. R. Soc.* A, **309,** 127.
[58] Kelly, S. M., 1994, *Liq. Crystals*, **17,** 211.
[59] Kelly, S. M., and Schadt, M., 1994, 23. *Freiburger Arbeitstagung Flüssige Kristalle.*
[60] Neises, B., and Steglich, W., 1978, *Angew. Chem.*, **90,** 556.
[61] Gerber, P., and Schadt, M., 1987, *Z. Naturf.* (*a*), **39,** 179.
[62] Österheld, G., Marugg, P., Rüher, R., and Germann, A., 1982, *J. Chrom.*, **234,** 99.
[63] Moia, F., and Schadt, M., 1990, *Digest SID Eurodisplay '90*, p. 132.
[64] Seiberle, H., and Schadt, M., 1994, *Molec. Crystals liq. Crystals*, **239,** 229.